ESR Investigation into the effects of heat treatment and crystal structure on radicals produced over irradiated TiO₂ powder

Yasuhiro Nakaoka, Yoshio Nosaka *

Department of Chemistry, Nagaoka University of Technology, Nagaoka, Niigata 940-2188, Japan

Accepted 30 June 1997

Abstract

Electron spin resonance measurements were carried out at 77 K under irradiation for anatase TiO₂ powders treated by heating at various temperatures in the air. For the untreated powder photoproduced holes were trapped at the surface forming $Ti^{4+}O^- \cdot Ti^{4+}OH^-$ radicals, while, for the heated powder, they were trapped as $Ti^{4+}O^{2-}Ti^{4+}O^-$ radicals at the surface. Photoproduced electrons were trapped as Ti^{3+} at the surface of the unheated powder, while they trapped at the inner part of the heat-treated powder. These differences could be explained by the desorption of surface hydroxyl groups and the change in the surface structure accompanied by the crystalline growth. No photoproduced radicals were detected for rutile TiO₂ powder, which may explain the low photocatalytic activity of this crystalline structure.   © 1997 Elsevier Science S.A.

Keywords: Photocatalyst; TiO₂; ESR; Radical

1. Introduction

Titanium dioxide (TiO₂) has been studied extensively as a photocatalyst [1,2]. Application of photocatalytic reactions with TiO₂ to environmental purification is promising because TiO₂ has an excellent chemical stability and the positive holes photogenerated on it have strong oxidation power [3]. The photocatalytic activity of TiO₂ strongly depends on its preparation conditions. It has been reported that the activity of photocatalysis is affected by the conditions of heat treatment as well as by the crystalline structure which is changed by the heat treatment from anatase to rutile [4–6]. For obtaining useful TiO₂ powders, the basic investigation into the differences of photocatalytic activity on the heat treatment should be clarified.

In the process of photocatalysis, the electrons and holes generated in the irradiated TiO₂ particles are trapped at the surface, forming paramagnetic species. The photocatalytic reactions arise from the reaction of these radicals with some reactant molecule at the TiO₂ surface. Electron spin resonance (ESR) spectroscopy has been used for detecting photoproduced radicals on TiO₂ [7–14]. The photogenerated electrons may be trapped at several sites; titanium atoms on the surface or inside the particles, or oxygen molecules adsorbed on the surface. The photogenerated holes were reported to be trapped at the oxygen atoms in the crystalline lattice near the particle surface or at hydroxyl groups on the surface. However, no report has clarified the difference in the photoproduced radicals based on the difference in the heat-treatment conditions and the crystalline structures.

We have been studying photoproduced radicals on photocatalysts such as CdS [15] and ZnS [16] by means of ESR spectroscopy. In the present work, we observed many photoproduced radicals on various TiO₂ powders treated with several temperatures, and the effects of heat treatment and crystalline structures on the photoproduced radicals over TiO₂ powder have been investigated.

2. Experimental details

The TiO₂ powders used were mainly Hombikat UV100 obtained from Sachtleben Chemie GmbH as a generous gift. This powder is one of the commercially available TiO₂ powders of 100% anatase. For comparison, TiO₂ powders purchased from Aldrich Chemicals and High Pure Chemicals were also employed. The powder of UV100 TiO₂ was heated in air at various temperatures ranging from 200°C to 1000°C for 5 h. XRD analyses were carried out with a Rigaku RAD III A X-ray diffractometer. For the ESR measurements, the TiO₂ powder was placed in a sample tube, and then it was evacuated to 1×10^{-3} Torr and sealed. In order to test the

* Corresponding author.

reactivity of the radicals observed on the powders, 1 atm of air, 45 Torr of 2-propanol vapor, or 20 Torr of water vapor was introduced into the sample tube. The ESR measurements were carried out at 77 K with a JEOL ES-RE2X ESR spectrometer under the photoirradiation of a 500 W mercury lamp (Ushio USH 500 D) through a bandpass filter (Toshiba UV-D36C). The recorded spectra were taken into a personal computer with an image scanner and converted to a g value scale referring to a Mn^{2+} marker. In some cases where the signal was small, the photoinduced ESR spectrum was obtained by subtracting the spectrum obtained in the dark from that obtained under the irradiation.

3. Results

3.1. XRD analysis of anatase TiO_2 powder with heat treatment

Fig. 1 shows variation in the X-ray diffractograms for the UV100 TiO_2 powders which were heated at various temperatures. The crystalline structure of the powders remains to be anatase below 850°C. The rutile structure clearly appeared for the samples heated at 900°C and the anatase structure completely disappeared at 1000°C. This observation shows that the phase transition of UV100 TiO_2 occurs in the temperature range from 850°C to 1000°C. The peaks of the X-ray diffractogram became sharp with increasing treatment temperature, showing the increase in the crystallite size.

3.2. ESR measurements for untreated powder

Fig. 2 shows the ESR spectra obtained from unheated TiO_2 powder under the irradiation. On the degassed sample there appeared mainly two signals, which are labeled as signals A and B (Fig. 2(a)). They are characterized by the sets of g values, $g_1 = 2.004$, $g_2 = 2.014$, $g_3 = 2.018$ and $g_\parallel = 1.957$,
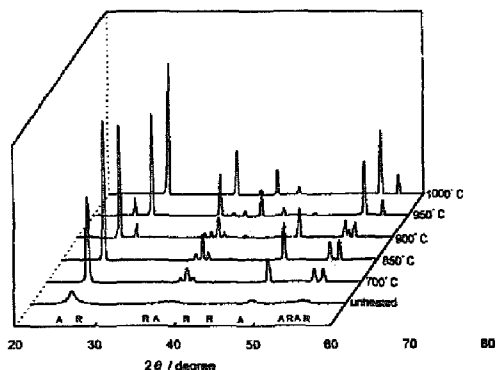
Fig. 1. X-ray diffractograms of UV100 TiO_2 powders heated at various temperatures for 5 h. A and R represent the peaks of anatase and rutile, respectively.
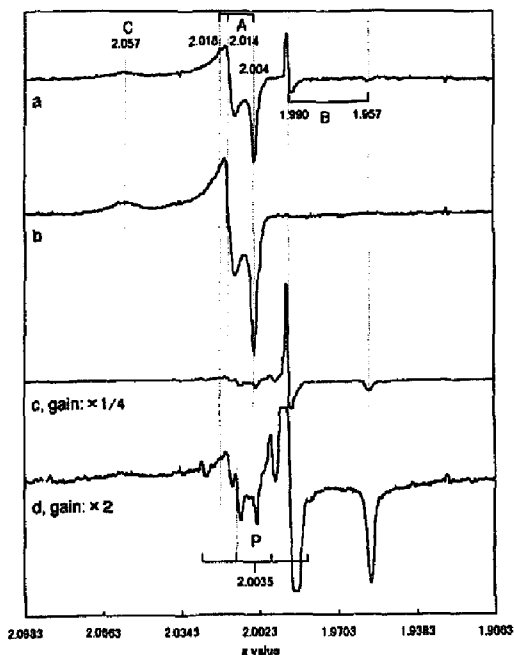
Fig. 2. ESR spectra obtained under the irradiation at 77 K for UV100 TiO_2 powder in vacuum (a), under air (b), and under 2-propanol vapor (c and d).

$g_\perp = 1.990$, respectively. Another broad signal also appeared at around $g = 2.06$, which is labeled as signal C.

In the presence of air, where the adsorbed oxygen molecule takes the role of an electron acceptor, the intensity of the signals A and C increased (Fig. 2(b)). On the other hand, under the 2-propanol vapor, which acts as a hole acceptor, the intensity of the signals A and C decreased and a new signal (signal P) appeared as shown in Fig. 2(c) and 2(d). The signal P consists of four isotropic signals at the intensity ratio of 1:3:3:1 with the hyperfine coupling constant of 2.3 mT. We assigned the signal P to methyl radicals, because these features agree well with that reported in the literature [17]. Although the 2-hydroxy-2-propyl radical is usually produced with the photocatalytic oxidation of 2-propanol as reported previously for CdS [15], the observed was a methyl radical for TiO_2. The details of the oxidation mechanism are not clear at the present time. These experimental results show that signal A is the trapped radicals of the photoinduced positive holes which can oxidize 2-propanol by forming a methyl radical, signal P. Signal C will be assigned in the later discussion.

On the other hand, signal B disappeared with the air (Fig. 2(b)) and increased in the presence of 2-propanol by an order of magnitude (Fig. 2(c) and 2(d)). Then, signal B may originate from trapped electrons on the particle surface where the electrons could participate in the photocatalytic reactions.
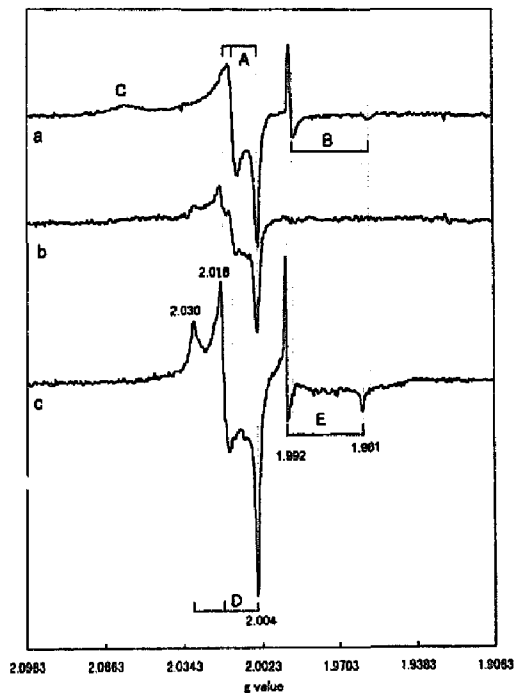
Fig. 3. ESR spectra measured at 77 K for irradiated UV100 TiO$_2$ powder unheated (a), heated at 350°C (b), and at 700°C (c) for 5 h.

Fig. 4. ESR spectra for UV100 TiO$_2$ powder heated at 700°C recorded at 77 K under irradiation in vacuum (a), with air (b), with 2-propanol vapor (c), and with water vapor (d).

3.3. Change in ESR signals by heat treatment

Fig. 3 shows the ESR spectra measured at 77 K under vacuum for the TiO$_2$ powders heated at various temperatures. Signal A decreased gradually with increasing temperature of heat treatment and almost completely disappeared at 700°C. Newly appeared in the heat treated TiO$_2$ was signal D of $g_1 = 2.004$, $g_2 = 2.018$, and $g_3 = 2.030$. The intensity of signal D became a maximum for the powder heated at 700°C and gradually decreased for those at a higher temperature. Under the air and the 2-propanol vapor signal D almost disappeared on the 700°C treated powder, as shown in Fig. 4. These observations indicate that the radicals giving signal D are formed at or near the surface.

Signal B was not observed for the powder heated at 200°C, but at 500°C a similar signal, labeled E, appeared at $g_{||} = 1.961$ and $g_{\perp} = 1.992$. The intensity of signal E became a maximum at 700°C and gradually decreased with increasing temperature. Since the signal intensity was not much affected by the existence of donor or acceptor molecules, the radical giving signal E was probably formed inside the particle. This signal was observed from the sample heated above 500°C, where the crystal size increased considerably. This experimental result shows that trapping sites of the charge carrier were formed inside the particles with the increase of the crystal size by the heat treatment.

It is notable that all these changes in the ESR signals occurred by heat treatment below 800°C where the crystalline
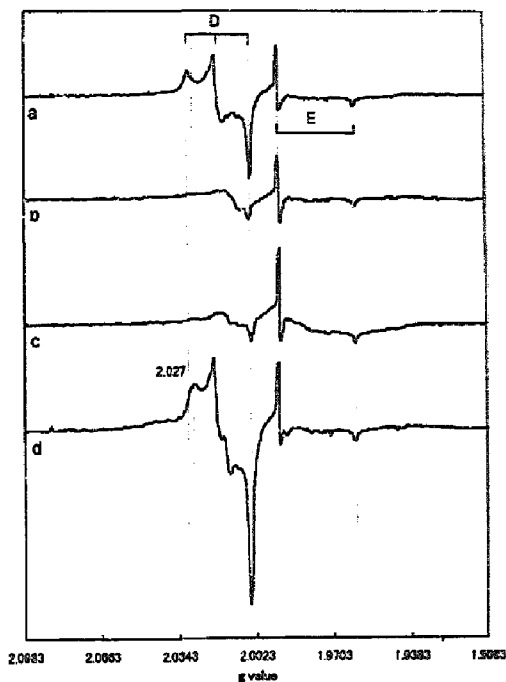
structure remained as anatase. Then, these changes were not caused by the alternation of the crystalline structures. This observation is different from the case of CdS where the crystalline structure significantly reflects on the ESR signals [15].

In order to examine the effect of the desorption of adsorbed water or a surface hydroxyl group, ESR measurements were carried out for the samples with water vapor. For the unheated powder, neither signals A nor B showed significant change by the addition of water vapor and no additional signal appeared. This observation suggests that the unheated powder was originally covered with water molecules. For the sample heated at 700°C, signal D changed in the g_3 component from 2.030 to 2.027 with water vapor as shown in Fig. 4. This change is probably due to the change in the spin distribution of radicals which may be caused by the adsorption of the water molecules. The change in g_3 also shows that the radicals corresponding to signal D lie at the particle surface. For the sample heated at 350°C and 500°C, the intensity of signal A increased with the addition of water vapor as shown in Fig. 5, although the intensity of signal A decreased with heat treatment. This experimental result is explained by the recovery of water molecules or surface hydroxyl group which has been desorbed by the heat treatment. As shown in Fig. 4(d), signals A and B observed for the unheated powder were not recovered with water vapor for the heated samples which gave signals D and E. Therefore, heat treatment caused not only the desorption of water molecules from the surface but
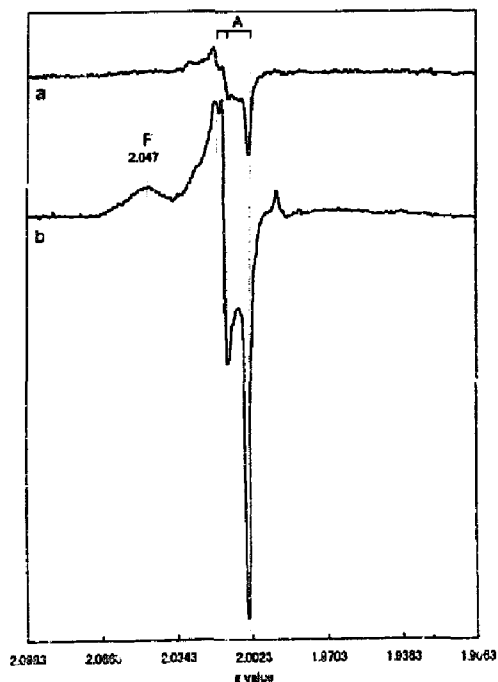
Fig. 5. ESR spectra for UV100 TiO₂ powder heated at 350°C recorded at 77 K under irradiation in vacuum (a), and with water vapor (b)

Fig. 6. Thermogravimetry curve for untreated UV100 TiO₂ powder.

also a certain change of the sample conditions including the surface structure.

The new signal, F, at around $g = 2.047$ appeared when water vapor was added to the powder heated at 200–700°C. This signal F may concern water molecules.

The thermogravimetry measurement of Fig. 6 shows that the weight of UV100 TiO₂ powder decreases up to 500°C by two steps. Although the initial fast decrease is attributed to the desorption of water, the weight loss at high temperature seems to be caused by the desorption of hydroxyl group. This observation indicates the existence of a hydroxyl group even at 500°C and supports the appearance of signal A which is concerned with the hydroxyl group.

The effects of heat treatment on the photoinduced radicals could be described as follows. Since the surface of the unheated UV100 TiO₂ powder is covered with water molecules and hydroxyl groups, the radicals photoproduced on the particle surface by the trapping of the photoinduced holes give the signal A. This radical concerns the surface hydroxyl group and has oxidation ability. Under these conditions, photogenerated electrons were trapped on the particle surface and gave the signal B. By heating the powder, the radicals of signal A become difficult to produce because of the desorption of the surface hydroxyl groups. This radical, however, could be reproduced when the surface hydroxyl group was recovered by the addition of water vapor. The desorption of the hydroxyl group may be accompanied by the growth of
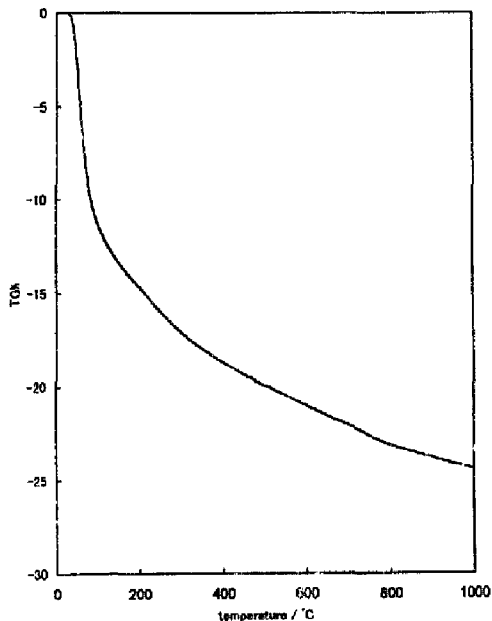
the crystals, which may cause some change in the surface structure. Thus, the radicals of signals D and E were produced on the heated particle. On increasing the heat-treatment temperature, the surface hydroxyl groups were thoroughly desorbed and the surface structure was changed significantly, because the signals A and B have not been recovered by the addition of water vapor.

3.4. Correlation between crystalline structure and photoproduced radicals

Figs. 7 and 8 show the X-ray diffractograms and the ESR spectra obtained from UV100 TiO₂ powder heated at 1000°C and TiO₂ powders of other sources. The UV100 TiO₂ powder becomes completely rutile at 1000°C. The ESR signal obtained for it was small and was not changed on the addition of electron donor nor acceptor molecules. Other TiO₂ powders (Aldrich and High Pure Chemicals) are originally rutile and almost no signal appeared on photoirradiation, even on the addition of electron donor and acceptor molecules. Therefore, it may conclude that the formation of photoinduced radicals is difficult on rutile TiO₂ powder. This experimental result corresponds to the low photocatalytic activity for most rutile powder. The rutile structure is a high-temperature stable phase and the heat treatment may be conducted in the preparation procedure by the manufacturers. By the heat treatment, the crystallite grows in size and the surface structure may be altered. Thus, the number of surface trapping sites decreases. These changes may be responsible for the difficulty in the photoformation of radicals on the rutile powders.
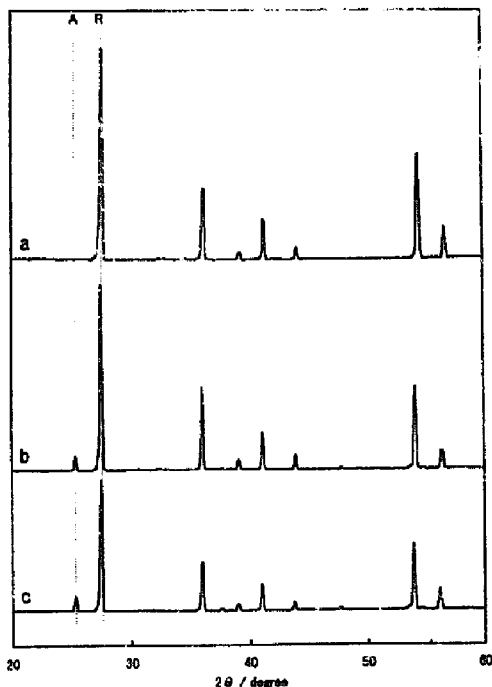
Fig. 7. X-ray diffractograms of UV100 TiO₂ powder heated at 1000°C for 5 h (a), Aldrich TiO₂ powder (b), and High Pure Chemicals TiO₂ powder (c).
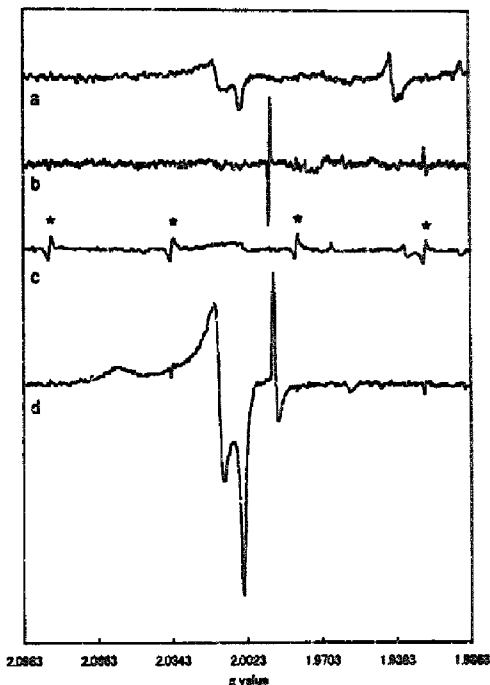

Fig. 8. ESR spectra obtained in vacuum at 77 K for UV100 TiO₂ powder heated at 1000°C for 5 h (a), Aldrich TiO₂ powder (b), High Pure Chemicals TiO₂ powder (c), and unheated UV100 TiO₂ powder (d). * represents Mn^{2+} marker.

4. Discussion

4.1. Hole trapping site

Signal A was attributed to the holes trapped on or near the particle surface, because, as shown in Fig. 2, the intensity of the signal decreased in the presence of electron donor molecules and increased in the presence of electron acceptor molecules. Moreover, the intensity of signal A decreased with heat treatment (Fig. 3) but it increased on the addition of water vapor (Fig. 5). These observations indicate that signal A is related to the surface hydroxyl group. On the other hand, signal D is not related to the surface hydroxyl group because it was observed only in the heated samples (Fig. 3). Signal D corresponds to the radicals produced on the surface of the particle, because the g value was changed by the addition of water vapor and then these radicals are sensitive to the environmental changes (Fig. 4). It has been reported that surface water is not oxidized by the surface trapped holes [11].

The oxygen radical O^- is known to be formed on the TiO₂ by the trapping of the photoproduced holes. The g values of the oxygen radicals were reported in the range from 2.00 to 2.03. Thus, signals A and D could be attributable to oxygen radicals. Table 1 lists the reported g values for oxygen radicals.

Howe and Grätzel reported that the photoproduced holes are trapped at the lattice oxygen atoms located in the subsur-

face layer of the hydrated anatase [9]. This radical has the structure of $Ti^{4+}O^- Ti^{4+}OH^-$ and has the set of g values of $g_1 = 2.002$, $g_2 = 2.012$ and $g_3 = 2.016$. Signal A corresponds well to this signal in the g values and the shape, and the surfaces of these samples are covered with hydroxyl groups. From this consideration, we assigned signal A to the $Ti^{4+}O^- Ti^{4+}OH^-$ radical.

Micic et al. reported the radical formation of trapped holes on the surface of TiO₂ colloid and its assignment to the $Ti^{4+}O^{2-} Ti^{4+}O^-$ radical [11]. The g values of the signal of this radical are reported to be $g_1 = 2.007$, $g_2 = 2.018$ and $g_3 = 2.027$. Signal D agrees well with this radical in respects of the set of g values, the location being affected by adsorbed molecules, and the absence of a surface hydroxyl group. From this observed evidence, we can assign signal D to the $Ti^{4+}O^{2-} Ti^{4+}O^-$ radical.

In the presence of 2-propanol vapor, the $Ti^{4+}O^- Ti^{4+}OH^-$ radical yielded a methyl radical (Fig. 2(c)) while no reaction occurred for the $Ti^{4+}O^{2-} Ti^{4+}O^-$ radical (Fig. 4(c)). This observation shows that the surface hydroxyl group acts as an important role in the oxidation of 2-propanol on the TiO₂ surface. Presumably, it takes a role of the adsorption of alcohols on the surface. Thus, the reactivity of these two radicals may be different from each other.

Table 1
The g values of oxygen and related radicals

Radicals	g value			Ref.
	g_1	g_2	g_3	
O^- (rutile + Ga)	2.007	2.023	2.030	[18]
O^- (rutile + Al)	2.003	2.019	2.026	[18]
O^- (V center, TiO_2 surface)	2.004	2.016	2.028	[19]
O^- (in MgO)	2.002	2.042	2.042	[20]
O^- (in ZnO)	2.0026	2.021	2.021	[21]
$Ti^{4+}O^- Ti^{4+}OH$ (hydrated anatase)	2.002	2.012	2.016	[9]
$Ti^{4+}O^{2-}Ti^{4+}O^-$	2.0073	2.0188	2.0273	[11]
OH (in H_2O ice)	2.0027	2.009	2.059	[22]
OH (on TiO_2 surface)	2.0032	2.0146	2.0146	[7]
O_2H	2.002	2.008	2.034	[13]
$Ti_nO^- Ti^{4+}OH^-$	2.030	2.030	2.030	[10]
O_2^- (on TiO_2, adsorbed oxygen)	2.003	2.009	2.025	[23]
O_2^- (on TiO_2, adsorbed oxygen)	2.001	2.009	2.021	[24]
O_2^- (on ZnO, adsorbed oxygen)	2.002	2.008	2.051	[25]
O_2^- (on zeolites, adsorbed oxygen)	2.004	2.009	2.057	[26]

4.2. Electron trapping site

Figs. 2 and 3 show that signal B appeared only on the unheated sample. It was found that signal B originates from the electrons trapped at the particle surface because the intensity increased with the presence of the electron donor molecules and decreased with the electron acceptor molecules (Fig. 2). Signal E has g values which are close to those of signal B. However, signal E appeared in the heated samples and showed no response to the presence of molecules (Fig. 4). Then, the radicals of signal E are assigned to the electrons trapped in the inner part of the particles which could not participate in the surface reactions.

It was reported that Ti^{3+} is formed on TiO_2 powders by trapping the photogenerated electrons. The g values of Ti^{3+} were reported to be below 2. Since the g values of both signals B and E are below 2, these two signals are attributable to Ti^{3+}. Table 2 lists the reported g values of trapped electrons at TiO_2. The difference between the g values of the surface Ti^{3+} and those of the inside Ti^{3+} are very small. Although it is difficult to predict the location of the Ti^{3+} radicals only from the g values, signal B could be assigned to the surface Ti^{3+} and signal E to the inner Ti^{3+} from the reactivity of these radicals. The fact that signal B disappeared for the sample heated at 200°C indicates that it arises from the non-stoichiometric surface Ti atoms of the initial powders. By the heat treatment at above 500°C, non-stoichiometric Ti atoms may be formed again at the grain boundary of the growth particle and they become an electron trapping site. In the photocatalysis on TiO_2, most reduction could not proceed unless metals have been deposited on TiO_2 surface as an electron trap [2,28,29]. It is probable that, in the absence of the deposited metal, the Ti^{3+} formed inside particles acts as an recombination center and reduces the activity of the surface reactions for heat-treated TiO_2 powders.

Signal C appeared at around $g = 2.06$ on the unheated sample as described above. This signal increased under air for the samples heated at 200°C and 350°C. Signal C may relate to adsorbed oxygen molecules, because it could not be observed essentially without the addition of air. Then, we assigned signal C to O_2^-, because the $g_\perp$ values of O_2^- radicals produced on ZnO and zeolite are reported to be 2.051 and 2.057, respectively [25,26]. Although the small signal was observed for the sample under vacuum in Fig. 2(a), a

Table 2
The g values of Ti^{3+} radicals

Radicals	g values			Ref.
	g_1	g_2	g_3	
Ti^{3+} (anatase + Nb)	1.962	1.992	1.992	[27]
Ti^{3+} (hydrated anatase)	1.960	1.990	1.990	[9]
Ti^{3+} (interstitial, coloidal TiO_2)	1.957	1.988	1.988	[8]
Ti^{3+} (surface, coloidal TiO_2)	1.885	1.925	1.925	[8]
Ti^{3+} (surface, coloidal TiO_2)	1.885	1.930	1.930	[8]
Ti^{3+} (surface, coloidal TiO_2)	1.880	1.945	1.945	[8]
$Ti(H_2O)_6^{3+}$	1.988	1.892	1.892	[4]
$Ti^{3+}VoTi^{4+}$	1.965			[10]

Table 3
The assignments of the signals obtained in this work

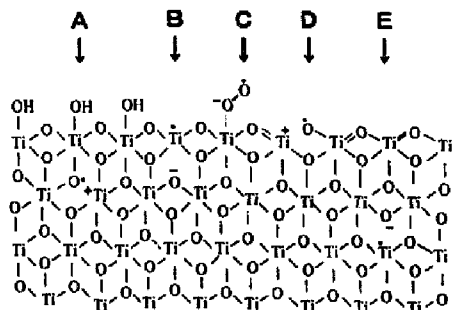| Signals	g_1	g_2	g_3	Assignment
A	2.004	2.014	2.018	$Ti^{4+}O^- Ti^{4+}OH^-$
B	1.957	1.990	1.990	surface Ti^{3+}
C	a	a	2.06	adsorbed oxygen, O_2^-
D	2.004	2.018	2.030	$Ti^{4+}O^{2-}Ti^{4+}O^-$
E	1.961	1.992	1.992	inner Ti^{3+}
F	a	a	2.047	adsorbed water

a Not distinguished.

Fig. 9. Plausible chemical structure for the radicals observed on anatase TiO$_2$ by means of ESR spectroscopy. A, trapped hole with OH group; B, surface trapped electron; C, adsorbed superoxide radical; D, surface trapped hole; E, inner trapped electron.

slight amount of adsorbed oxygen molecules had not been removed without heat treatment.

Table 3 summarizes the g values and assignments of the ESR signals obtained from photoirradiated TiO$_2$ powders. The plausible chemical structures are illustrated in Fig. 9 for two types of trapped holes (A and D) and two types of trapped electrons (B and E).

5. Conclusions

In the present work, we have shown that when anatase TiO$_2$ powder was heat-treated the photoproduced radicals were altered. The change in the radicals is caused by the desorption of surface hydroxyl group and the consequential change in the surface structure. In the unheated samples possessing surface hydroxyl group, photogenerated holes produce the Ti^{4+}O$^-$·Ti^{4+}OH$^-$ radicals as reported by Howe and Grätzel [9]. The photogenerated electrons produce the Ti^{3+} radicals at the surface. Both radicals could participate in the photocatalytic reaction with the surrounding molecules. On the other hand, when the hydroxyl group has been desorbed by heat treatment, the photogenerated holes produce the Ti^{4+}O^{2-}·Ti^{4+}O$^-$· radicals as reported by Micic et al. [11]. This radical shows a different reactivity from the Ti^{4+}O$^-$·Ti^{4+}OH$^-$ radical. The photogenerated electrons in the heat-treated TiO$_2$ powder produce Ti^{3+} radicals in the inner part of the particles and could not participate in the surface reaction. These differences in the photoproduced radicals cause the different reactivity of the TiO$_2$ powders treated at different heating temperatures. On rutile TiO$_2$ powders, it is difficult to produce such radicals, corresponding to the poor photocatalytic activity of most rutile powders.

References

[1] N. Serpone, E. Pelizzetti (Eds.), Photocatalysis: Fundamentals and Applications, Wiley, New York, 1989.
[2] A.L. Linsebigler, G. Lu, J.T. Yates, Jr., Chem. Rev. 95 (1995) 735.
[3] M.R. Hoffmann, S.T. Martin, W. Choi, D.W. Bahnemann, Chem. Rev. 95 (1995) 69.
[4] R.C. Wilson, R.J. Myers, J. Chem. Phys. 64 (1974) 2208.
[5] S. Nishimoto, B. Ohtani, H. Kajiwara, T. Kagiya, J. Chem. Soc., Faraday Trans. 1 81 (1985) 61.
[6] B. Ohtani, S. Nishimoto, J. Phys. Chem. 97 (1993) 920.
[7] M. Anpo, I. Shima, Y. Kubokawa, Chem. Lett. (1985) 1799.
[8] R.F. Howe, M. Grätzel, J. Phys. Chem. 89 (1985) 4495.
[9] R.F. Howe, M. Grätzel, J. Phys. Chem. 91 (1987) 3906.
[10] M. Avudaithai, T.R.N. Kutty, Mat. Res. Bull. 23 (1988) 1675.
[11] O.I. Micic, Y. Zhang, K.R. Cromack, A.D. Trifunac, M.C. Thurnauer, J. Phys. Chem. 97 (1993) 7277.
[12] O.I. Micic, Y. Zhang, K.R. Cromack, A.D. Trifunac, M.C. Thurnauer, J. Phys. Chem. 97 (1993) 13284.
[13] J. Soria, M.J. López-Munoz, V. Augugliaro, J.C. Conesa, Colloids and Surface A: Physicochemical and Engineering Aspects 78 (1993) 73.
[14] M.J. López-Munoz, J. Soria, J.C. Conesa, V. Augugliaro, in V.C. Corberán, S.V. Bellón (Eds.), New Developments in Selective Oxidation II, Elsevier Science, Netherland, 1994, p. 693.
[15] Y. Nakaoka, Y. Nosaka, J. Phys. Chem. 99 (1995) 9893.
[16] Y. Nakaoka, Y. Nosaka, Langmuir 13 (1997) 708.
[17] M. Kaise, H. Nagai, K. Tokuhashi, S. Kondo, Langmuir 10 (1994) 1345.
[18] D. Zwingel, Solid State Commun. 26 (1978) 775.
[19] A.R. Gonzalez-Elipe, G. Munuera, J. Soria, J. Chem. Soc., Faraday Trans. 1 75 (1979) 748.
[20] N.-B. Wong, J.H. Lunsford, J. Chem. Phys. 55 (1971) 3007.
[21] N.-B. Wong, Y.B. Taarit, J.H. Lunsford, J. Chem. Phys. 60 (1974) 2148.
[22] M.C.R. Symons, J. Chem. Soc., Faraday Trans. 1 78 (1982) 1953.
[23] C. Naccache, P. Meriaudeau, M. Che, A. Tench, J. Trans. Faraday Soc. 67 (1971) 506.
[24] P. Meriaudeau, J.C. Vedrine, J. Chem. Soc., Faraday Trans. 2 72 (1976) 472.
[25] J.H. Lunsford, J.P. Jayne, J. Chem. Phys. 44 (1966) 1487.
[26] P.H. Kasai, J. Chem. Phys. 43 (1965) 3322.
[27] J. Kiwi, J.T. Suss, S. Szapiro, Chem. Phys. Lett. 106 (1984) 135.
[28] H. Kominami, T. Matsuura, K. Iwai, B. Ohtani, S. Nishimoto, Y. Kera, Chem. Lett. (1995) 693.
[29] B. Ohtani, K. Iwai, H. Kominami, T. Matsuura, Y. Kera, S. Nishimoto, Chem. Phys. Lett. 242 (1995) 315.